THE UNIVERSITY OF MICHIGAN
DEPARTMENT OF ATMOSPHERIC, OCEANIC, AND SPACE SCIENCES
SPACE PHYSICS RESEARCH LABORATORY
2455 Hayward Street
Ann Arbor, Michigan 48109-2143

Contract/Grant Number:	NNG04GE64G
Project Name:	XMM-Newton X-Ray Observation of Jupiter
Project Director:	J. Hunter Waite
Report Date:	May 9, 2005
Report Type:	Summary of Research Report
Period Covered:	March 15, 2004 - March 14, 2005
Distribution:	Dr. Richard F. Mushotzky, Technical Officer NASA Goddard Space Flight Center Code 662 Greenbelt MD 20771 ONR Chicago John C. Kluczynski Federal Bldg. 230 S. Dearborn St., Suite 380 Chicago IL 60604-1595 Hanan A. Barrett, Grant Negotiator NASA Goddard Space Flight Center Code 210.G Greenbelt MD 20771 NASA Center for AeroSpace Information Attn: Document Processing Section 7121 Standard Dr. Hanover MD 21076 Kathy DeWitt UM DRDA File F010232/047577

XMM-Newton X-Ray Observation of Jupiter

NNG04GE64G (UM F010232/047577)

Summary of Research

May 9, 2005

The work carried out under this contract involves working with Dr. Tom Cravens to develop a model of the Jovian and Kronian x-ray disk emissions, which can be applied to the Chandra and XMM data sets. The enclosed draft of a paper represents a good summary of that work.

X-Ray Emission From the Outer Planets: Albedo for Scattering and Fluorescence of Solar X-Rays

T. E. Cravens and J. Clark
(University of Kansas)

A. Bhardwaj and R. Elsner
(Marshall Space Flight Center)

J. H. Waite, Jr.
(University of Michigan)

A. N. Maurellis
(Space Research Organization Netherlands)

L. W. Acton
(Montana State University)

G. R. Gladstone
(Southwest Research Institute)

DRAFT May 3, 2005 - still in progress

Abstract.

Soft X-ray emission has been observed from the disk of both Jupiter and Saturn as well as from the auroral regions of these planets. The low-latitude disk emission as observed by ROSAT, the Chandra X-Ray Observatory, and XMM-Newton appears to be uniformly distributed across the disk and to be correlated with solar activity. These characteristics suggest that the disk x-rays are produced by: (1) the elastic scattering of solar X-rays by atmospheric neutrals and (2) the absorption of solar X-rays in the carbon K-shell followed by fluorescent emission. The carbon atoms are found in methane molecules located below the homopause. In this paper we present the results of calculations of the scattering albedo for soft x-rays. We also show the calculated x-ray intensity for a range of atmospheric abundances for Jupiter and Saturn and for a number of solar irradiance spectra. The model calculations are compared with recent x-ray observations of Jupiter and Saturn. We conclude that the emission of soft x-rays from the disks of Jupiter and Saturn can be largely explained by the scattering and fluorescence of soft x-rays. We suggest that measured x-ray intensities from the disk regions of Jupiter

and Saturn can be used to determine both the absolute intensity and the spectrum of solar x-rays. X-ray observations of Jupiter and Saturn could then act as an important source of information on the solar soft x-ray flux.

1. Introduction

X-Ray emission has been observed from Jupiter with the Einstein satellite [*Metzger et al.*, 1983], the ROSAT satellite [*Waite et al.*, 1994, 1997; *Ness and Schmitt,* 2000], the XMM-Newton Observatory [*Branduari-Raymont et al.*, 2004; *Bhardwaj et al., 2005a*], and the Chandra X-Ray Observatory (CXO) [*Gladstone et al.*. 2002; *Elsner et al.*, 2005; *Bhardwaj et al.*, 2005b; *Ness et al*, 2004a,b]. The ROSAT observations indicated that the Jovian x-rays were predominantly soft (i.e., photon energies less than 1 keV or so) with both low-latitude and high-latitude (i.e., auroral) spatial components although these components were not spatially resolved [*Waite et al*, 1994, 1997; *Gladstone et al.*, 1998]. The total x-ray power was observed to be about 1 GW. The auroral emission has been attributed to energetic heavy ion precipitation [*Metzger et al.*, 1983; *Waite et al.*, 1994 ; *Horanyi et al.*, xxx; *Cravens et al..*, 1995; *Kharchenko*, xxx; *Liu and Schultz*, xxx; *Gladstone et al.*, 2002; *Cravens et al.*, 2003; *Elsner et al.*, 2005]. The origin of the low-latitude x-rays was not obvious, although *Gladstone et al.* [1998] demonstrated that the disk-integrated intensity appeared to correlate with the F10.7 proxy for solar extreme ultraviolet (EUV) radiation. *Maurellis et al.* [2000] proposed that the low-latitude Jovian x-ray emission could be explained by the scattering of solar x-ray photons by atmospheric neutrals and by fluorescent scattering of solar x-rays due to the carbon (in atmospheric methane) K-shell.

The CXO, with its much better spatial resolution than ROSAT, clearly revealed that the x-ray emission has two distinct components [*Gladstone et al.*, 2002]: (1) emission spread approximately uniformly over the disk (including low and mid-latitudes), and (2) auroral emission which is spatially very localized in the polar cap at latitudes higher than the main auroral oval. Both components had an emitted power of roughly 1 GW. More recent CXO observations have confirmed the existence of these two x-ray emission regions [*Elsner et al.*, 2004], as did recent XMM-Newton observations of Jupiter [*Branduari-Raymont et al.*, 2004]. Both CXO [*Bhardwaj et al.*, 2005a; *Elsner et al.*, 2005] and XMM- [*Branduari-Raymont et al.*, 2004] also obtained spectra of the auroral and disk x-rays, which were distinctly different. Recently, *Bhardwaj et al.* (2005a) demonstrated that the soft x-ray emission observed from Jupiter's disk with XMM were correlated with solar x-rays.

Saturn is also a source of soft x-rays, with emission observed at both low and high latitudes, although Saturn's x-ray luminoisty (about xxxxx MW) is much less than Jupiter's [*Ness et al*, 2004a,b]. *Ness and Schmitt* [2000] set upper limits for the x-ray emission from Uranus and Neptune. *Bhardwaj et al.* [2005b] recently presented CXO observations of an x-ray "flare" from Saturn that nicely correlates with a solar flare that should have been visible at Saturn as well as at Earth. *Bhardwaj* et al. [2005b] suggested that Saturn acted as "mirror" for solar x-rays and that this mirror effect could be used to detect flares from regions of the Sun not visible from the Earth. The purpose of the current paper is to follow up on the *Maurellis et al.* [2000] and *Bhardwaj et al.* [2005a,b] work by presenting model calculations for elastic scattering and K-shell fluoresence

scattering of solar x-rays from both Jupiter and Saturn. for a variety of conditions and assumed atmospheric compositions. In particular, we will explicitly calculate scattering albedos using the methods described in *Cravens and Maurellis* [2001] and *Maurellis et al.* [2000]. We suggest that measured x-ray intensities from the disk regions of Jupiter and Saturn can be used to determine both the absolute intensity and spectrum of solar x-rays. X-ray observations of Jupiter and Saturn could then act as an important source of information on the solar soft x-ray flux. The solar EUV and soft x-ray irradiance spectrum is a key input for aeronomical studies of the terrestrial and planetary upper atmospheres and ionospheres [e.g., *Schunk and Nagy*, 2000; *Nagy and Cravens*, xxxx; *Fox et al.*, xxxx; Barth xxxx].

2. Albedo for Scattering and Fluorescence of Solar X-Rays

X-rays can be both absorbed and elastically scattered (both incoherently and coherently – REF) by atoms or molecules in an atmosphere. The cross sections for these processes depend on wavelength (or photon energy). Figure 1 shows atomic cross sections for absorption and scattering for H, He, and C. The cross sections for H_2 and CH_4 were assumed to be the sum of the atomic cross sections in the soft x-ray part of the spectrum. The cross sections were taken from the NIST tabulations [*Chantler, 1995*]. Note that the scattering cross sections are much less than the absorption cross sections for the wavelengths under consideration in this paper.

Maurellis et al. [2000] calculated the intensity of solar x-rays scattered from Jupiter using these cross sections and using a model neutral atmosphere of Jupiter that included altitude profiles of molecular hydrogen, helium, and methane. The x-ray production rate

was determined at each wavelength and as a function of altitude. Optical depth effects for incoming and outgoing ray paths were included. The absorption of x-rays beyond the K-shell edge by carbon (in the methane) also results in X-ray emission due to K-shell fluorescence. This K-shell edge is apparent in Figure 1 at a wavelength near 4 nm [*Maurellis et al.* , 2000].

Cravens and Maurellis [2001] used a computationally simpler approach of finding x-ray scattering and fluorescence albedoes applied this method to x-ray production by Venus and Mars. We apply this method to Jupiter and Saturn in the current paper. The scattered x-ray intensity, $I_\lambda(\theta)$, at a given wavelength, λ, and scattering angle, θ, is the product of the solar flux at that wavelength (πF_λ, described later in section 4.) and the wavelength and angle dependent scattering albedo:

$$4\pi I_\lambda = A_\lambda(\theta)\ \pi F_\lambda \qquad (1)$$

where πF_λ is the solar flux at wavelength λ at the top of the atmosphere and $A_\lambda(\theta)$ is the scattering albedo. This albedo method is applicable if the atmospheric species mixing ratios are assumed to be uniform, which is true below the homopause. Figure 2 of *Maurellis et al.* indicates that the unit optical depth level is located below about 350 km for wavelengths $\lambda < 12$ nm, except for solar zenith angles close to 90° (i.e. near the limb). The homopause altitude on Jupiter is located at about 350 km [*c.f., Gladstone et al., 1996*]. The elastic scattering albedo derived by *Cravens and Maurellis* [2001] is:

$$A_\lambda(\theta) = \omega_\lambda^{tot}(\theta)\frac{1}{1+f_{io}} \qquad (1)$$

where the effective single scattering albedo is given by:

$$\omega_{\lambda}^{tot}(\theta) = \frac{\sum_{s} b_s 4\pi (d\sigma_{s,scatt}(\lambda,\theta)/d\Omega)}{\sum_{s} b_s \sigma_{s,abs}(\lambda)} \qquad (2)$$

$b_s = n_s / n_{tot}$ is the relative abundance of atomic species s (by volume), the number density of species s is n_s and the total number density is n_{tot}. The absorption cross section for species s is denoted $\sigma_{s,abs}(\lambda)$ and the differential scattering cross section for species s can be written as:

$$\sigma_{s,scatt}(\lambda,\theta) = \sigma_{s,scatt}(\lambda)(3/8\pi)\frac{1+\cos^2\theta}{2} \qquad (3)$$

$\sigma_{s,scatt}$ is the total scattering cross section. The scattering angle depends on the observing geometry as does the ratio of effective pathlengths, f_{io}. f_{io} is equal to the ratio of the Chapman functions for the incoming (to the Sun) and outgoing (to the Earth) zenith angles. For the outer planets the scattering angle is within a few degrees of 180°; we adopt $\theta = 180°$. Similarly, except right near the terminator, we can adopt $f_{io} = 1$ almost everywhere on the disks of the outer planets.

Cravens and Maurellis [2001] also derived an expression for the effective albedo for K-shell fluorescence and we have applied this expression to solar photon fluorescence from methane in this paper (we will not reproduce this expression here). Note that carbon K-shell photons are produced at energies close to .284 keV (or wavelengths near 4.3 nm).

Figures 2 – 4 show the calculated albedo for elastic scattering from equation (1) as a function of wavelength and for a range of abundances. Figure 2 shows the albedo for Jupiter and Saturn abundances (He/H_2 = 17 % and CH_4/ H_2 = 0.25 % by volume for Jupiter and He/H_2 = 6 % and CH_4/ H_2 = 0.2 % for Saturn). Note that the albedo increases with decreasing wavelength (or increasing energy) as expected from the behaviour of the cross sections (Fig. 1). The albedo is somewhat greater for Saturn than for Jupiter, mainly because the Jovian He abundance is higher and the He absorption cross section exceeds the hydrogen absorption cross section. The two scattering cross sections are similar. The carbon K-shell edge can be seen in the albedo curves near a wavelength of 4 nm.

Figures 3 and 4 display the albedo versus relative helium abundance and methane abundance, respectively, for 3 wavelengths. The albedo decreases with increasing helium abundance. Similarly, for wavelengths below the carbon K-shell edge, increasing methane abundance yields a lower albedo. This dependence on abundance suggests that the albedo (and scattered intensity) should be higher for observations right near the limb where the altitude of unit optical depth moves above the homopause height. The abundances of helium and methane relative to hydrogen rapidly decrease with altitude above the homopause.

3. Solar EUV and Soft X-Ray Fluxes

The intensity of x-rays scattered from a planet depends not only on the albedo but also on the incident solar radiation. The photon flux at a given wavelength (i.e., the solar

irradiance spectrum) is denoted πF_λ (see equation (1)). *Maurellis et al.* [2000] used low solar activity irradiances (for July 15, 1994) represented with 320 wavelength bins in the EUV and soft x-ray regions of the spectrum. For λ between 3 and 12 nm, the solar irradiances from the EUV97 solar proxy model [*Tobisca and Eparvier*, 1997] were used, but for the 0.2 – 3 nm region of the spectrum, *Maurellis et al.* [2000] used irradiances from modeled synthetic spectra [*Mewe et al.*, 1985; *Mewe and van den Oord*, 1986] that were themselves normalized with Yohkoh-derived coronal color temperatures [*Acton et al.*, 1999]. This solar flux will be referred to later in the paper as the low activity A flux and is shown in Figure 1 of *Maurellis et al.* [2000]. F10.7 = 85.7 for this case. We also use in this paper another low solar activity irradiance spectrum (for July 12, 1994) – denoted low activity flux B. For this case, the soft x-ray flux is somewhat lower but was derived with the same methods, but the irradiances for $\lambda > 3$ nm were taken from the more recent Solar2000 model [REF *tobisca*] (see Figure 5; denoted as "solar min,. B"). Figure 5 shows this irradiance spectrum. F10.7 = 83 for this case. The low activity B flux significantly exceeds the low activity A flux in the 3 – 5 nm part of the spectrum. A solar irradiance spectrum for "generic" high solar activity conditions was also constructed in the same manner, although there was some difference in the activity level we used for the soft x-ray and EUV portions of the spectrum. F10.7 = 233 for the EUV flux and F10.7 = 157 for the soft x-ray flux.

4. X-Ray Emission from the Outer Planets

Equation (1) can now be used to determine scattered x-ray intensities for Jupiter and Saturn. Scattered intensities for the low activity solar spectrum A were shown by *Maurellis et al.* [2000] for Jupiter. Similar results for the solar spectrum B are shown in Figure 6. The scattered x-ray flux was summed over 50 eV photon energy bins and (see Figure 7) for both the A and B low activity solar flux cases. These spectra do not include the carbon K-shell line intensities from the fluorescence mechanism. Note that the intensities shown in these Figures are for a situation in which Jupiter is located at a heliocentric distance of 1 AU. Obviously the actual Jovian x-ray intensities would be less by a factor of the heliocentric distance squared (i.e., $5^2 \approx 25$). The scattered intensity calculated for Saturn for the same solar conditions looks very much the same (and will not be shown), but Saturn is about twice as far from the Sun as Jupiter, so that the scattered intensity is smaller by about a factor of 4. In addition, the scattering albedo for Saturn is about 50% greater than the Jovian albedo.

Table 1 lists total (i.e., summed over wavelength) scattered x-ray intensities for both Jupiter and Saturn (actual distances) for several cases. Carbon K-shell line intensities are also listed in this table. For the low activity A solar flux, the K-shell contribution relative to the total scattering intensity is about 8%, whereas for the low activity B and high activity solar fluxes, the K-shell contribution is in the range 15 – 20%. This is because these solar flux spectra have rather high fluxes near 3 – 4 nm, just below the carbon K-shell edge. However, if one just considers the total power scattered, the elastically scattered intensity dominates over the K-shell contribution for all cases. Note that the solar flux A calculations using the albedo method agree with the *Maurellis et al.* [2000] results.

Table 2 lists total x-ray power densities as would be seen at Earth, both from our model and from various observations available in the literature. For simplicity, we have adopted Jovian and Saturnian heliospheric distances of 5.2 AU and 9.5 AU, respectively. We have also used these values for the Earth-planet distances. In fact, however, these distances can differ from these values by as much as 10% depending of the specific observational geometry, and this effect could have as much as 20% effect on the calculated powers. However, the current accuracy of the model and our limited knowledge of the input solar spectrum are undoubtedly worse than 20% at this time. For equivalent solar activity levels (i.e., for the same input solar flux levels), we find that the x-ray flux observed at Earth is $\approx$ 10 times less for Saturn than for Jupiter. A factor of $\approx$ 12 would be expected for identical albedos; the remaining difference is due to Saturn's somewhat higher scattering albedo.

Some measured x-ray powers for Jupiter and Saturn are also provided in Table 2. The values were located within their row of the Table according to the appropriate solar activity level (i.e., F10.7) with lower values being to the left. A more complete compilation of observed "disk" (i.e., non-auroral) x-ray powers for Saturn is provided by *Bhardwaj et al.* [2005b] who thus demonstrates a good correlation between x-ray production and solar activity. Such a solar activity dependence of the disk x-ray power is also evident in Table 2 for both planets.

5. X-Ray Spectra of the Disks of the Outer Planets

The scattered solar spectrum, like the incident solar spectrum, is expected to be contain discrete line emission from a very large number of atomic transitions. And given

that the solar flux is highly time-variable, especially in the x-ray part of the spectrum, then the Jovian and Saturnian disk spectra should also be highly time-variable. Disk spectra have been measured for Saturn (*Ness et al.*, 2004a,b; *Branduari-Raymont et al.*, 2004). These spectra show particularly high count rates in the 0.6 to 1 keV part of the planetary disk spectra, which is consistent with the model spectra shown earlier. For Jupiter, the disk spectra measured by XMM-Newton (*Branduari-Raymont et al.*, 2004) differ substantially from the spectra observed in the auroral regions [*Elsner et al.*, 2005]. The auroral intensities are (relatively) much higher near energies of 0.6 keV and 0.3-0.4 keV than are the disk spectra (*Branduari-Raymont et al.*, 2004; *Elsner et al.*, 2005). The Jovian and Saturnian disk spectra are quite similar.

In this paper, we show comparisons of model disk spectra with spectra measured by the Chandra ACIS-S instrument. Figure 8 shows these comparisons for both the solar flux A ("old solar min.") and solar flux B ("new solar min.") model cases for Jupiter. Figure 9 shows comparisons for Saturn. The Chandra spectrum for Jupiter was taken on Februrary 24, 2003. A detailed discussion of these measurements will be presented in another (companion) paper now in preparation [*Bhardwaj et al.*]. The model intensities used in these figures were the 50 eV average values (see Fig. 7), convolved with the ACIS-S energy-dependent instrumental response (area) function. The carbon K-shell line intensities were included.

The spectra measured for Jupiter and Saturn are very similar in their general shape, as are the modeled spectra, although there is disagreement on the smaller energy scales. In particular, the predicted spectra and measured count rates/intensities for both planets are relatively high for photon energies between 0.2 and 0.4 keV and between 0.7 and 0.9

keV. The intensities are lower near .4 keV and above 1 keV. The solar flux A model agrees better with the data than does the solar flux B case, particularly near an energy of 0.4 keV. The two models differ only in the two solar flux models used. The model/data agreement also appears to be somewhat better for Saturn (Figure 9) than for Jupiter (Figure 8). Again, as either the disk spectra already in the literature, and discussed earlier, the measured spectra in Figures 8 and 9 differ greatly from the measured Jovian auroral x-ray spectra.

5. Discussion and Conclusions

Maurellis et al. (2000) proposed that the low-latitude soft x-ray emission from Jupiter could be explained by the scattering of solar x-rays. Several characteristics of the observed x-ray emission from the disks of Jupiter and Saturn support this suggestion. First, the non-auroral x-ray intensities observed from Jupiter or Saturn appear to be at least approximately uniform *(Gladstone et al*, 2002; *Elsner et al.,* 2004; *Branduari-Raymont et al.*, 2004; *Ness et al.*, 2004a,b; *Bhardwaj et al.*, 2005a), as would be predicted by equation (1) for an outer planet for which both the factor f_{io} and the scattering angle, θ, do not vary much across the disk. Second, the disk intensities appear to correlate with the solar x-ray flux, or at least with the F10.7 proxy index of solar activity (*Gladsone et al.*, 1999; *Maurellis et al.*, 2000; *Bhardwaj et al.*, 2005a,b). Third, as mentioned in the previous section, the Jupiter-Saturn intensity ratio is roughly what one would expect for a solar-related mechanism. Fourth, the observed disk x-ray spectra for Jupiter and Saturn are largely consistent with scattered solar x-rays.

Ness and Schmitt [2000] used ROSAT observations to set 95% confidence upper limits to the soft x-ray energy flux from Uranus and Neptune of 5.7×10^{-15} and 4.7×10^{-15} ergs cm^{-2} s^{-1}, respectively. With the assumption that all the emission from these planets is due to scattered solar x-rays (and using Jovian albedo values and the high solar activity solar flux case), we predict soft x-ray fluxes from Uranus and Neptune of 1.3×10^{-16} and 2.0×10^{-17} ergs cm^{-2} s^{-1}, respectively. These values are much less than the *Ness and Schmitt* [2000] upper limits for these planets.

Solar extreme ultraviolet and soft x-ray photons are a major energy source for the upper atmospheres and ionospheres of most solar system bodies [*Schunk and Nagy*, 2000]. Quoting from page 241 of *Schunk and Nagy* [2000]: "Solar radiation in the EUV and x-ray range of wavelengths excites, dissociates, and ionizes the neutral consitutents in the upper atmosphere." Hence, the solar EUV and x-ray flux plays an important role in the field of aeronomy. A number of solar flux models have been used over the years (c.f., *Schunk and Nagy*, 2000), but a continuing need exists for better and more accurate solar flux data, partly because the solar flux is so highly variable and because the spectrum is so complex (*Tobisca and Barth*, 1990; *Hinteregger et al.*, 1981; *Tobisca and Eparvier*, 1998; *Warren et al*, 2001).

In this paper we determined the soft x-ray emission from the disks of Jupiter and Saturn using both existing EUV solar flux data (*Tobisca*, 1998) and collisional equilibrium models of the solar corona combined with Yohkoh observations of the Sun (*Acton et al.*, 1999). The scattered radiation in our models depends on these solar flux values and on the scattering albedo. It might also be useful to use the observations of the Jovian and Saturnian disk emission by CXO and XMM to provide information on the

solar soft x-ray flux. That is, Jupiter and Saturn could be used as mirrors (albeit low reflectivity mirrors), as suggested by *Bhardwaj et al.* [2005b]. Oversimplifying what the procedure would need to be, the solar irradiance spectrum could be 'measured' simply by dividing the measured Jovian or Saturnian intensity by the scattering albedo at a given photon energy or wavelength. Of course, a complication is introduced by the need to fold in energy-dependent sensitivity factors of the specific observatory/instrument. The alternative procedure is a standard one used for analysis of CXO and XMM spectra and the one we used in Figures 8 and 9 – that is, to fit the data to models with a certain number of fitting parameters, in which case the model intensities are "run through" the machinery accounting for instrumental sensitivity (e.g,. *Elsner et al*, 2005; *Branduari-Raymont et al.*, 2004). But either way, a solar soft x-ray spectrum versus energy could be derived for different solar conditions using the Jovian or Saturnian x-ray observations. For this paper, we did this in only a crude way (that is, we can conclude that our solar flux A model appears to be more appropriate than the solar flux B model, at least for the times that the CXO observations were made). This new solar information could serve as an important supplement to the current sources of information, and could, on occasion, provide information on the solar flux being generated from regions of the solar disk not visible from the Earth.

6. References

Acton, L. W., D. C. Weston, and M. E. Bruner, Deriving solar X ray irradiance from *Yohkoh* observations, *J. Geophys. Res.*, *104*, 14827, 1999.

Bhardwaj, A., et al., Soft X-ray emissions from planets, moons, and comets, *ESA-SP-514*, 215-226, 2002.

Bhwardwaj, A., G. Branduardi-Raymont, R. F. Elsner, G. R. Gladstone, G. Ramsay, P. Rodriguez, R. Soria, J. H. Waite, Jr., and T. E. Cravens, Solar control on Jupiter's equatorial emissions : 26-29 November 2003 XMM-Newton Observation, *Geophysical Res. Lett.*, *32*, L03SXX, doi :1029/2004GL021497, 2005a.

Bhardwaj, A., R. F. Elsner, J. H. Waite, Jr., G. R. Gladstone, T. E. Cravens, and P. Ford, X-ray flare and aurora at Saturn, *Ap. J. Lett,xxxxx, 2005b.*

Branduardi-Raymont, G., et al. , First observation of Jupiter by XMM-Newton, *Astron. Astrophys.*, *424*, 331-337, 2004.

Chantler, C. T., Theoretical form factor, attenuation, and scattering tabulation for Z = 1-92 from E= 1-10 eV to E= 0.4 –1.0 MeV, *J. Phys. Chem. Ref. Data*, **24**, 71, 1995.

Cravens, T. E., E. Howell, J. H. Waite, and G. R. Gladstone, Auroral oxygen precipitation at Jupiter, *J. Geophys. Res.*, *100*, 14827, 1995.

Cravens, T.E., and A.N. Maurellis, X-ray emission from scattering and fluorescence of solar x-rays at Venus and Mars, *Geophys. Res. Lett.*, *28*, 3043-3046, 2001.

Cravens, T.E., et al., Implications of Jovian X-ray emission for magnetosphere-ionosphere coupling, *J. Geophys. Res.*, *108* (A12), 1465, doi:10.1029/2003JA010050, 2003.

Elsner, R.F., et al., Simultaneous Chandra X-ray, HST ultraviolet, and Ulysses radio observations of Jupiter's aurora, *J. Geophys. Res.*, xxxx, doi: 10.1029/2004JA010717, 2005.

Gladstone, G.R., J.H. Waite, Jr., and W.S. Lewis, Secular and local time dependence of Jovian X ray emissions, *J. Geophys. Res.*, *103*, 20083–20088, 1998.

Gladstone, G. R., et al., A pulsating auroral X-ray hot spot on Jupiter, *Nature*, *415*, 1000-1003, 2002.

Maurellis, A.N., T.E. Cravens, G.R. Gladstone, J.H., Waite, and L.W. Acton, Jovian X-ray emission from solar X-ray scattering, *Geophys. Res. Lett.*, *27*, 1339-1342, 2000.

Metzger, A. E. et al., The detection of X rays from Jupiter, *J. Geophys. Res.*, *88*, 7731, 1983.

Mewe, R., E. H. N. M. Gronenschild, and G. H. J. van den Oord, Calculated X-radiation from optically thin plasmas, Paper V, *A & A Suppl.*, *62*, 197-254, 1985.

Ness, J.-U., J. H. M. M. Schmitt, A search for X-ray emission from Saturn, Uranus, and Neptune, *Astronomy and Astrophysics*, *335*, 394, 2000.

Ness, J.-U., J. H. M. M. Schmitt, S. J. Wolk, K. Dennerl, and V. Burwitz, X-ray emission from Saturn, *Astronomy and Astrophysics*, *418*, 337, 2004a.

Ness, J.-U., J. H. M. M. Schmitt, and J. Robrade, Detection of Saturnian X-ray emission with XMM-Newton, *Astronomy and Astrophysics*, *414*, L49, 2004b.

Tobisca, W. K., and F. G. Eparvier, EUV97: Improvements to EUV irradiance modeling in the soft X rays and FUV, *Solar Physics*, *177*, 147, 1998.

Waite, J. H., Jr., et al., ROSAT observations of the Jupiter aurora, *J. Geophys. Res.*, *99*, 14799, 1994.

Waite, J.H., Jr., et al. (1997), Equatorial X-ray emissions: Implications for Jupiter's high exospheric temperatures, *Science*, *276*, 104-108.

Table 1.

Spectrally Summed Soft X-Ray Intensities for Jupiter and Saturn at 1 AU Calculated with the Model

4π I (R)

Source (wavelength)	*low activity A*	*low activity B*	*high activity*
JUPITER			
elastic (0.2 – 12 nm)	0.51	1.26	3.79
Carbon K-shell (4.4 nm)	0.028	0.20	0.68
Total	0.54	1.46	4.47

Note: *Maurellis et al* low activity A case: total intensity = 0.56 R

SATURN			
elastic (0.2 – 12 nm)	0.77	1.89	5.62
Carbon K-shell (4.4 nm)	0.037	0.26	0.90
Total	0.81	2.15	6.52

Note: 1 Rayleigh (R) = 10^6 cm^{-2} s^{-1} and the units of intensity are cm^{-2} s^{-1} sr^{-1}

Table 2.

Total Soft X-Ray Fluxes From Jupiter and Saturn as Observed at Earth: Model Results and Observations

Power Density (10^{-14} ergs cm^{-2} s^{-1})

Source (energy)	*low activity A F10.7 = 83*	*low activity B F10.7 = 86*	*high activity F10.7 = 157-233)*
JUPITER			
elastic (.10 – 1.7 keV) (no K-shell)	2.49	4.88	16.2
(.10 – 1.7 keV) (with K-shell)	2.59	5.59	18.6
elastic (.3 – 1.7 keV)	1.52	3.22	11.8
XMM disk[1] (.3 – 2 keV)		4.	
ROSAT [2] (.1 - .55 keV; disk = 50% total)			15
SATURN			
elastic (.10 – 1.7 keV) (no K-shell)	0.25	0.50	1.66
(.10 – 1.7 keV) (with K-shell)	0.26	0.57	1.89
elastic (.3 – 1.7 keV)	0.14	0.31	0.66
XMM[3] (.1 – 2 keV; disk)		1.6	
CXO[4] (.1 – 2 keV; disk)	0.5	0.68	1.2
ROSAT[2] ((.1 - .55 keV; all)			1.9

1. *Branduardi-Raymont, et al,* [2004].
2. *Ness and Schmitt* [2000].
3. *Ness et al.* [2004a].
4. *Ness et al.* [2004b].

FIGURES

Figure 1. Elastic scattering and aborption cross sections as a function of wavelength for H, He, and C. From the NIST tabulations [*Chantler, 1995*].

Figure 2. Elastic scattering albedo for Jupiter and Saturn versus wavelength. The scattering angle is assumed to be 180° (appropriate for the Earth and the planet being in opposition).

Figure 3. Elastic scattering albedo versus the fractional He to H_2 abundance for Saturnian methane abundance (the results for the Jovian methane abundance are almost the same). The albedo is shown for 3 wavelengths.

Figure 4. Elastic scattering albedo versus the methane abundance for a Saturnian helium abundance.

Figure 5. Solar irradiance spectra at 1 AU for low solar activity (denoted low activity B spectrum in the text.)

Figure 6. Scattered Jovian x-ray intensity (normalized for 1 AU) versus wavelength at high resolution. The spectrum does not include the carbon K-shell line intensities from the fluorescence mechanism.

Figure 7. Scattered Jovian x-ray intensity (normalized for 1 AU) versus photon energy at 50 eV resolution for 2 different low solar activity solar fluxes. The spectrum does not include the carbon K-shell line intensities from the fluorescence mechanism.

Figure 8. Comparison of measured and modeled disk x-ray spectra for Jupiter. The modeled count rates for the top panel are for the solar flux A case ("old min"). The bottom panel is for the solar flux B case ("new min"). The model intensities are processed using the CXO ACIS-S instrumental response function in order to generate modeled instrumental count rates. The models include the carbon K-shell line intensities. The data shown are from CXO ACIS-S measurements of Jupiter during February 2002 (see the companion paper by *Bhardwaj, A., et al, 2005,* for details of the observations; the auroral data from this same set of CXO observations was described in *Elsner et al.*, 2005).

Figure 9. Same as Figure 8 but for the Saturn disk. The solar flux A case was used for the model. The data are CXO ASIS-S measurements taken during xxxxx, date (REF??).

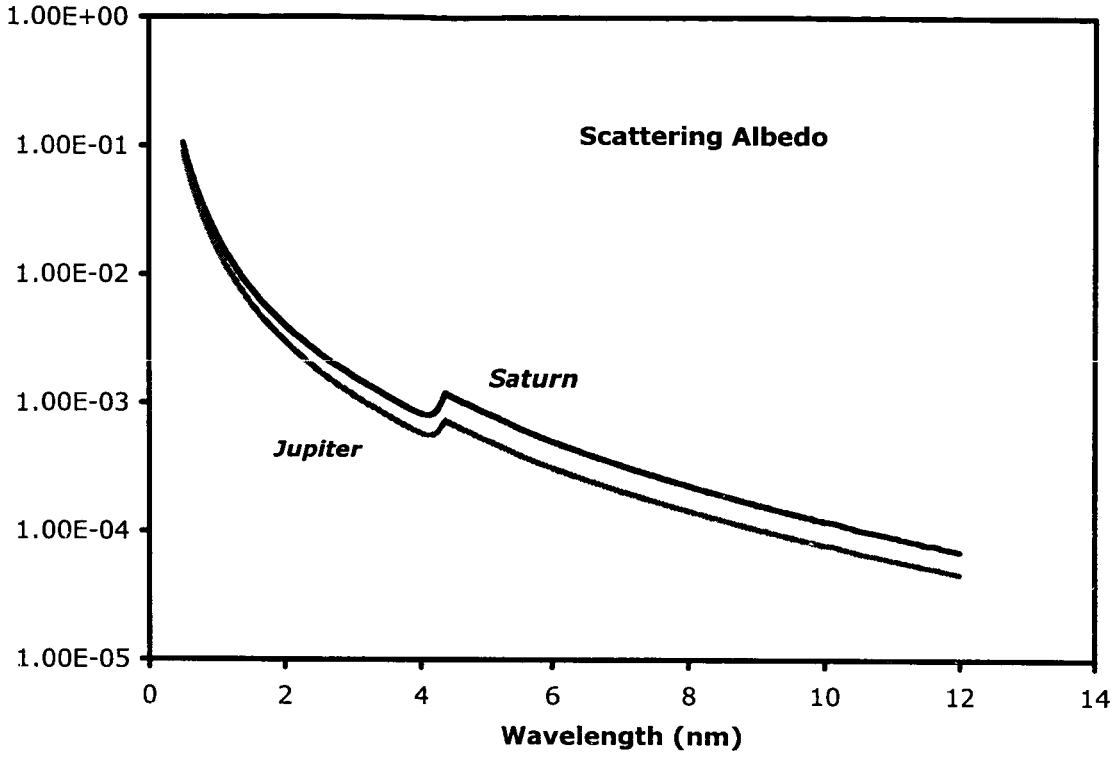

Figure 2.

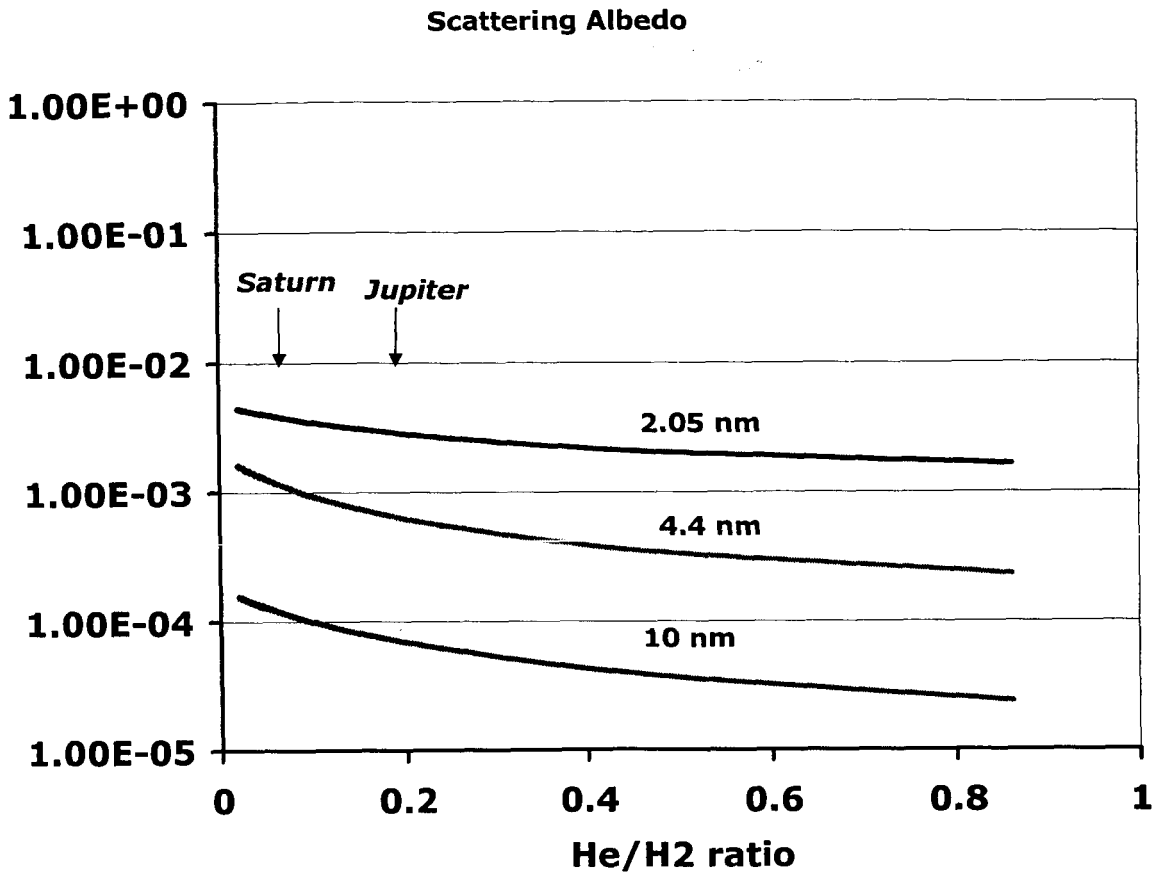
Scattering Albedo
1.00E+00
1.00E-01
1.00E-02
1.00E-03
1.00E-04
1.00E-05
Saturn
Jupiter
2.05 nm
4.4 nm
10 nm
0
0.2
0.4
0.6
0.8
1
He/H2 ratio

Figure 3.

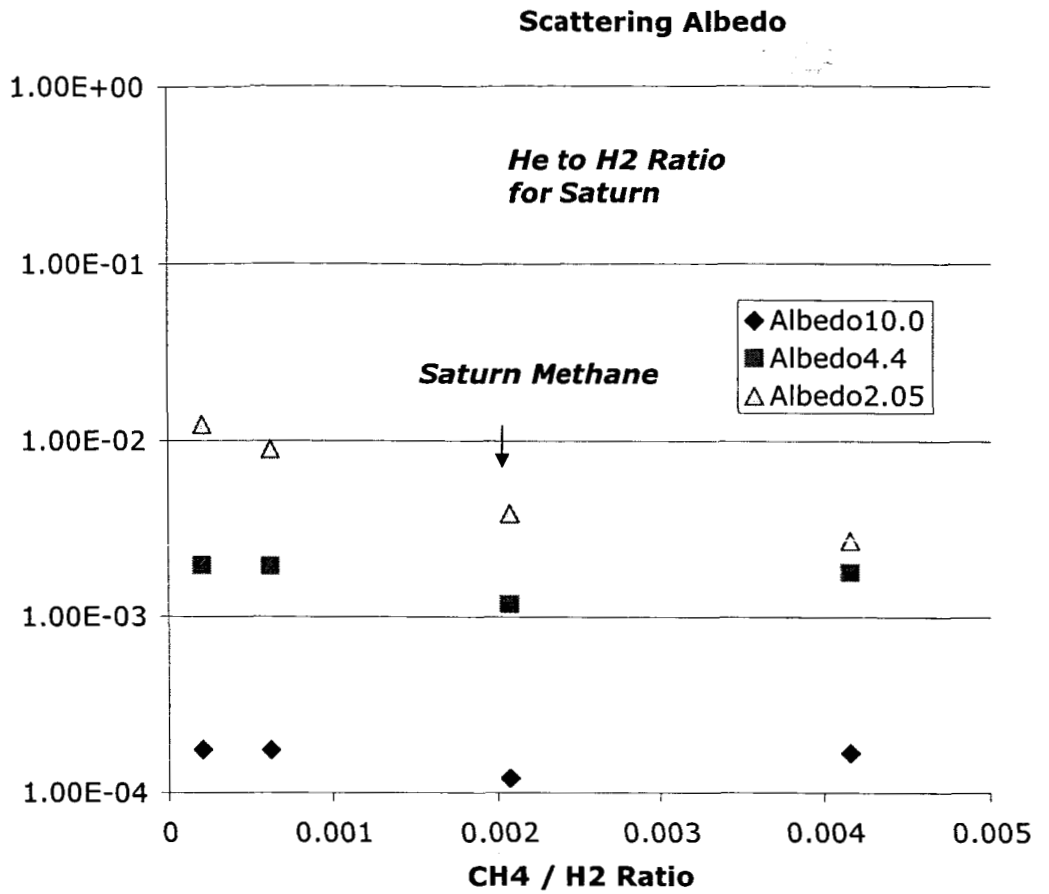
Scattering Albedo
1.00E+00
1.00E-01
1.00E-02
1.00E-03
1.00E-04
He to H2 Ratio
for Saturn
Saturn Methane
Albedo10.0
Albedo4.4
Albedo2.05
0
0.001
0.002
0.003
0.004
0.005
CH4 / H2 Ratio

Figure 4.

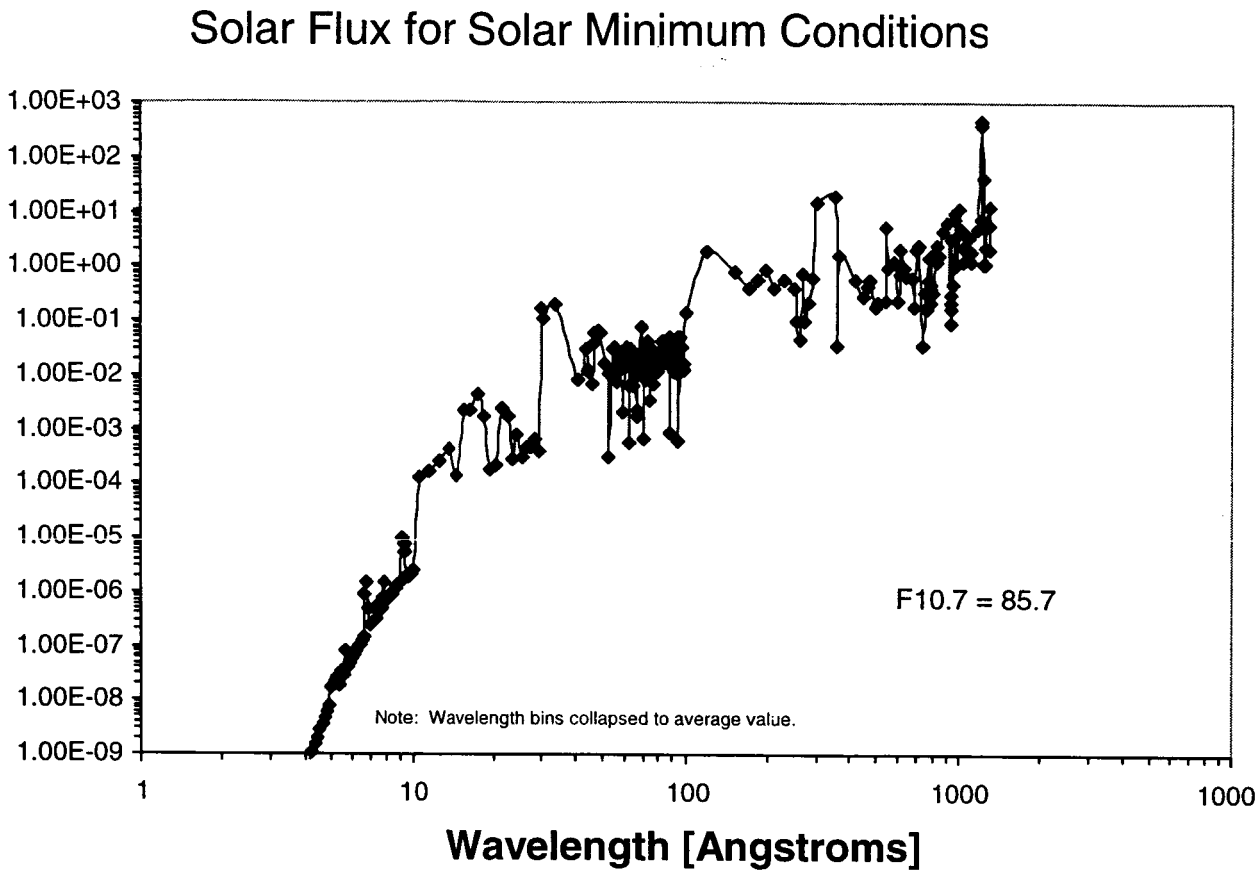
Solar Flux for Solar Minimum Conditions
1.00E+03
1.00E+02
1.00E+01
1.00E+00
1.00E-01
1.00E-02
1.00E-03
1.00E-04
1.00E-05
1.00E-06
1.00E-07
1.00E-08
1.00E-09
F10.7 = 85.7
Note: Wavelength bins collapsed to average value.
1
10
100
1000
1000
Wavelength [Angstroms]

Figure 5.

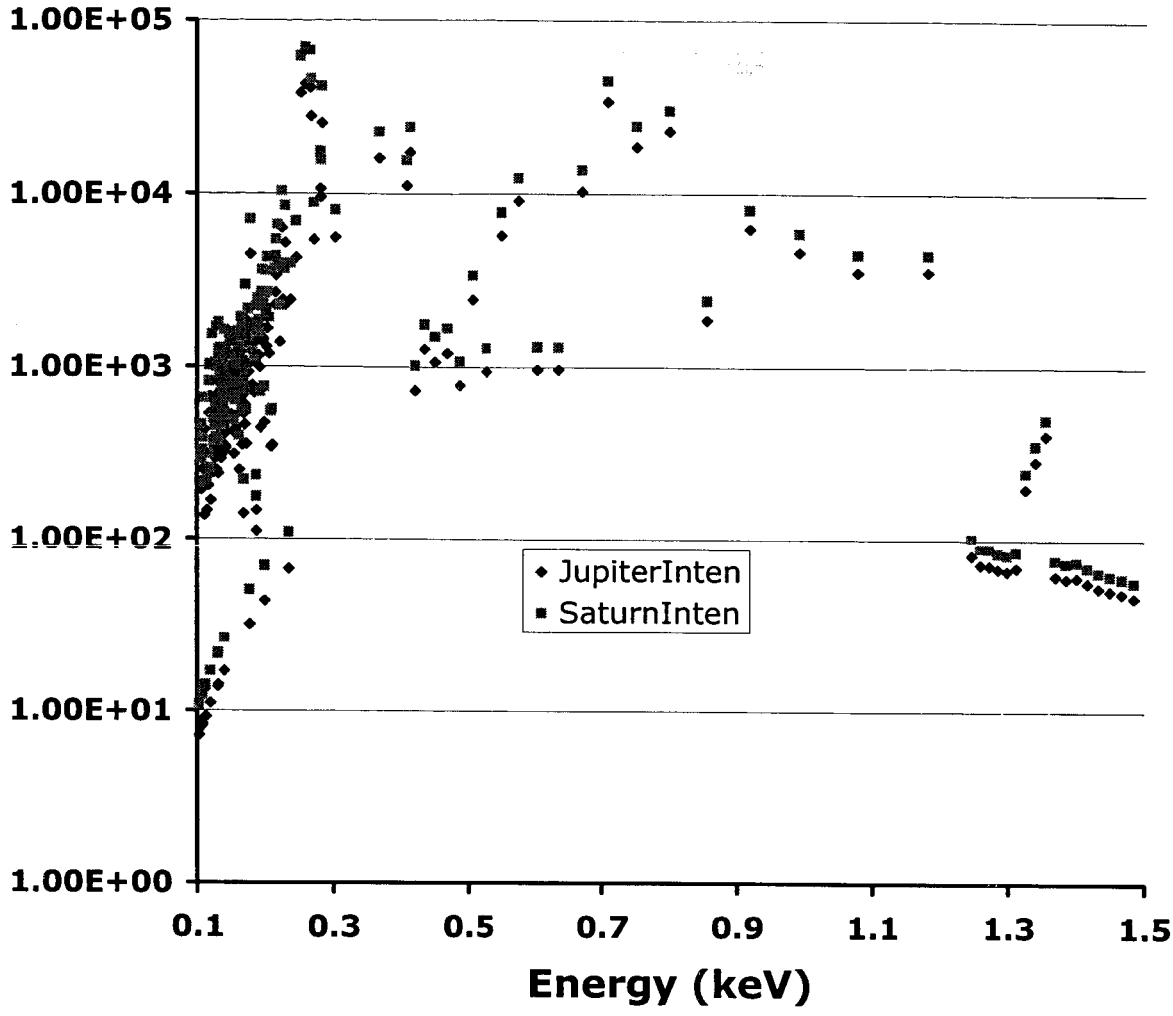
1.00E+05
1.00E+04
1.00E+03
1.00E+02
1.00E+01
1.00E+00
0.1
0.3
0.5
0.7
0.9
1.1
1.3
1.5
Energy (keV)
JupiterInten
SaturnInten

Figure 6.

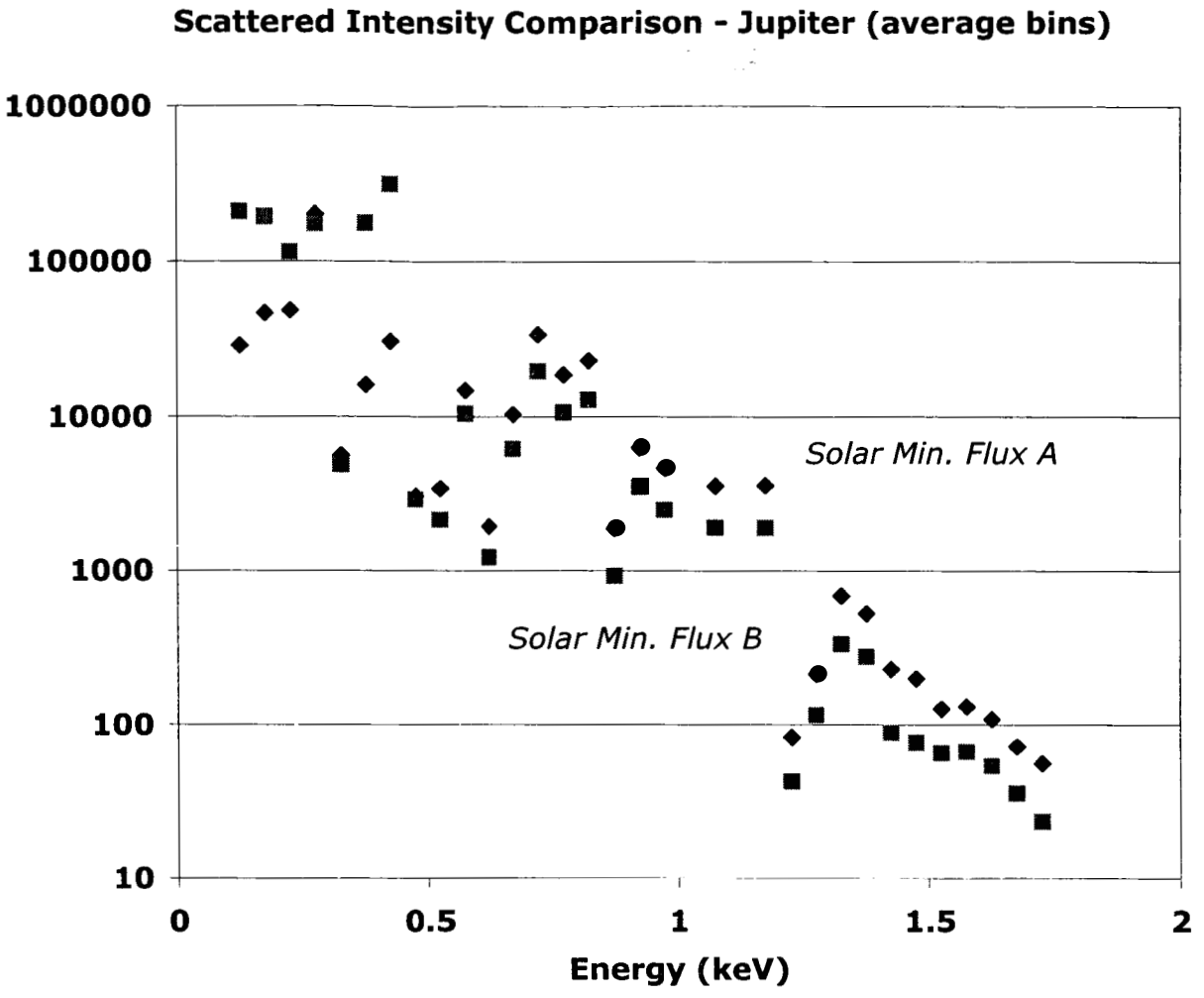
Scattered Intensity Comparison - Jupiter (average bins)
1000000
100000
10000
1000
100
10
0
0.5
1
1.5
2
Energy (keV)
Solar Min. Flux A
Solar Min. Flux B

Figure 7.

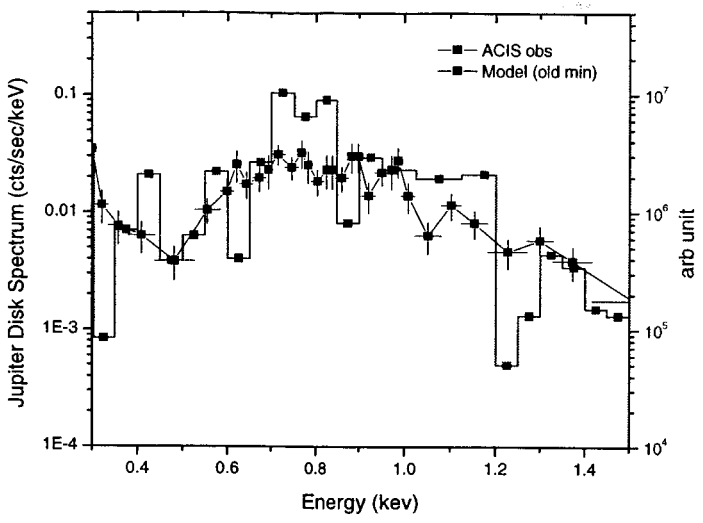
ACIS obs
Model (old min)
Jupiter Disk Spectrum (cts/sec/keV)
arb unit
Energy (kev)

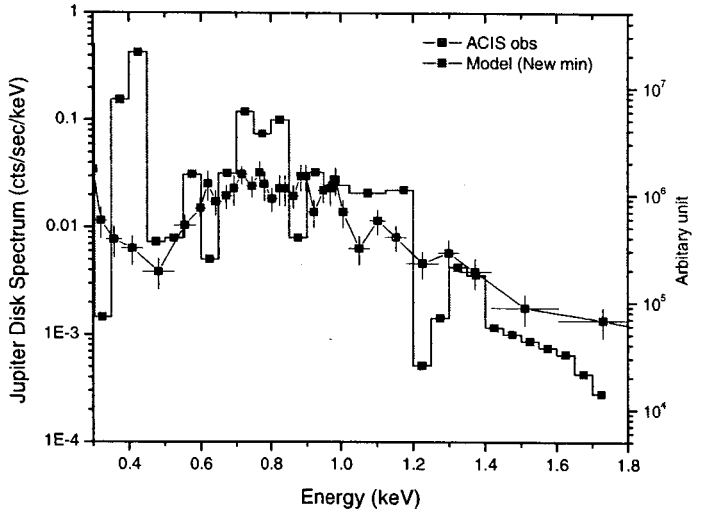
ACIS obs
Model (New min)
Jupiter Disk Spectrum (cts/sec/keV)
Arbitary unit
Energy (keV)

Figure 8.

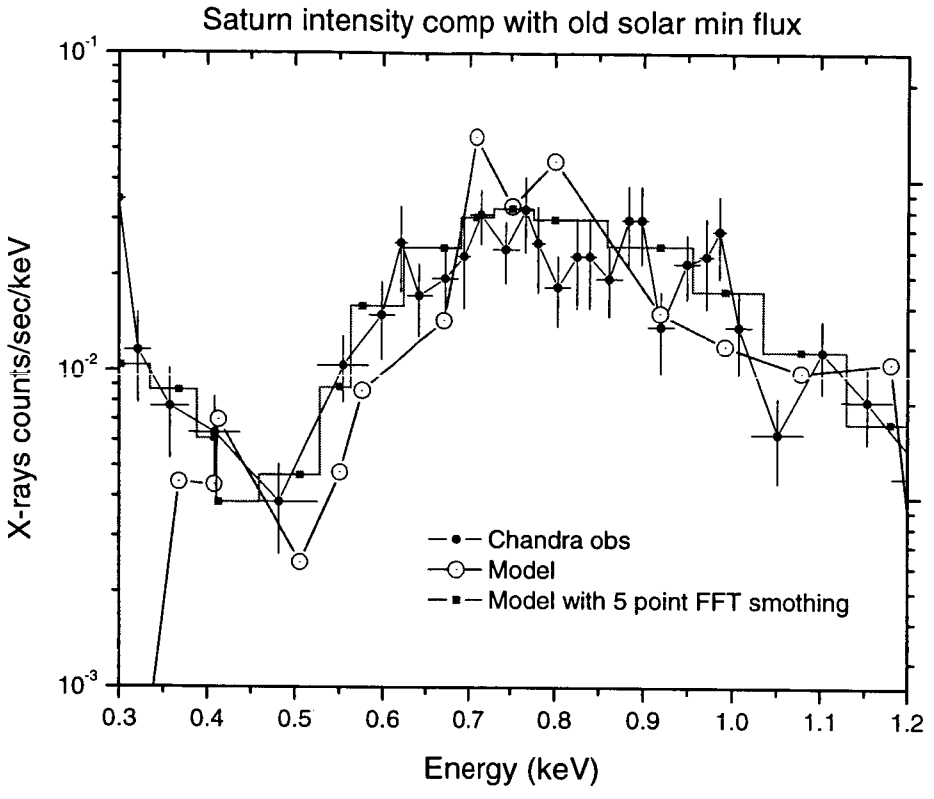
Saturn intensity comp with old solar min flux
X-rays counts/sec/keV
Energy (keV)
Chandra obs
Model
Model with 5 point FFT smothing

Figure 9.